

advances.sciencemag.org/cgi/content/full/6/29/eaba8105/DC1

Supplementary Materials for

Cryo-EM structures of calcium homeostasis modulator channels in diverse oligomeric assemblies

Kanae Demura, Tsukasa Kusakizako, Wataru Shihoya, Masahiro Hiraizumi, Kengo Nomura, Hiroto Shimada, Keitaro Yamashita, Tomohiro Nishizawa, Akiyuki Taruno*, Osamu Nureki*

*Corresponding author. Email: taruno@koto.kpu-m.ac.jp (A.T.), nureki@bs.s.u-tokyo.ac.jp (O.N.)

Published 17 July 2020, *Sci. Adv.* **6**, eaba8105 (2020)
DOI: 10.1126/sciadv.aba8105

This PDF file includes:

Figs. S1 to S11
Table S1

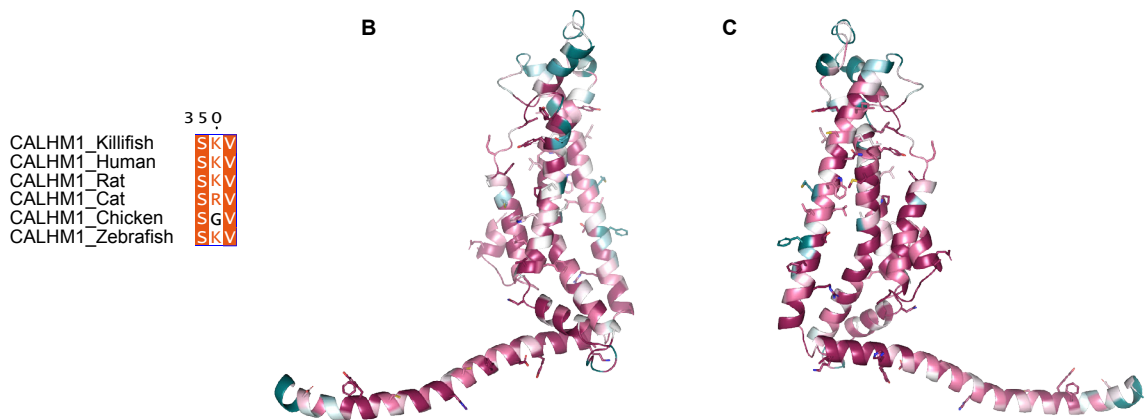
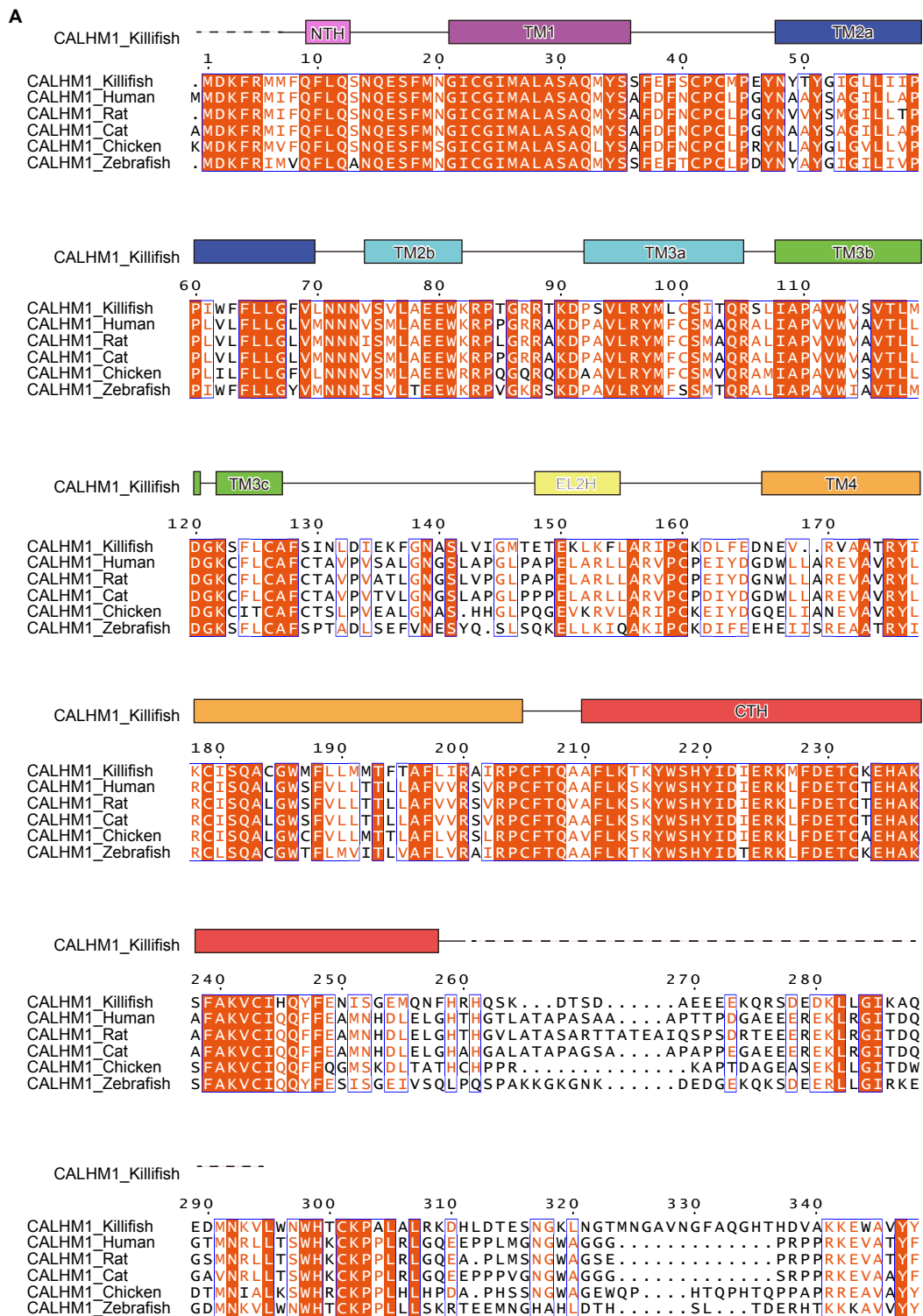


Fig. S1: Amino acid sequence alignment of the CALHM1 orthologs.

(A) Alignment of the amino-acid sequences of killifish CALHM1 (OICALHM1, UniProt ID: H2MCM1), human CALHM1 (UniProt ID: Q8IU99), rat CALHM1 (UniProt ID: D4AE44), cat CALHM1 (UniProt ID: M3VYF2), chicken CALHM1 (UniProt ID: A0A1D5NWS1), and zebrafish CALHM1 (UniProt ID: E7F2J4). Secondary structure elements for α -helices are indicated by cylinders. Conservation of the residues is indicated as follows: red panels for completely conserved; red letters for partly conserved; and black letters for not conserved. (B and C) Conservation of the residues of CALHM1 family members. The sequence conservation among 384 CALHM1 orthologs was calculated using the ConSurf server (<http://consurf.tau.ac.il>), and is colored from cyan (low) to maroon (high). The residues constituting the subunit interface are indicated by stick models. They are conserved in the CALHM1 orthologs, except for Met187 and Phe194, which are exposed to the membrane environment.

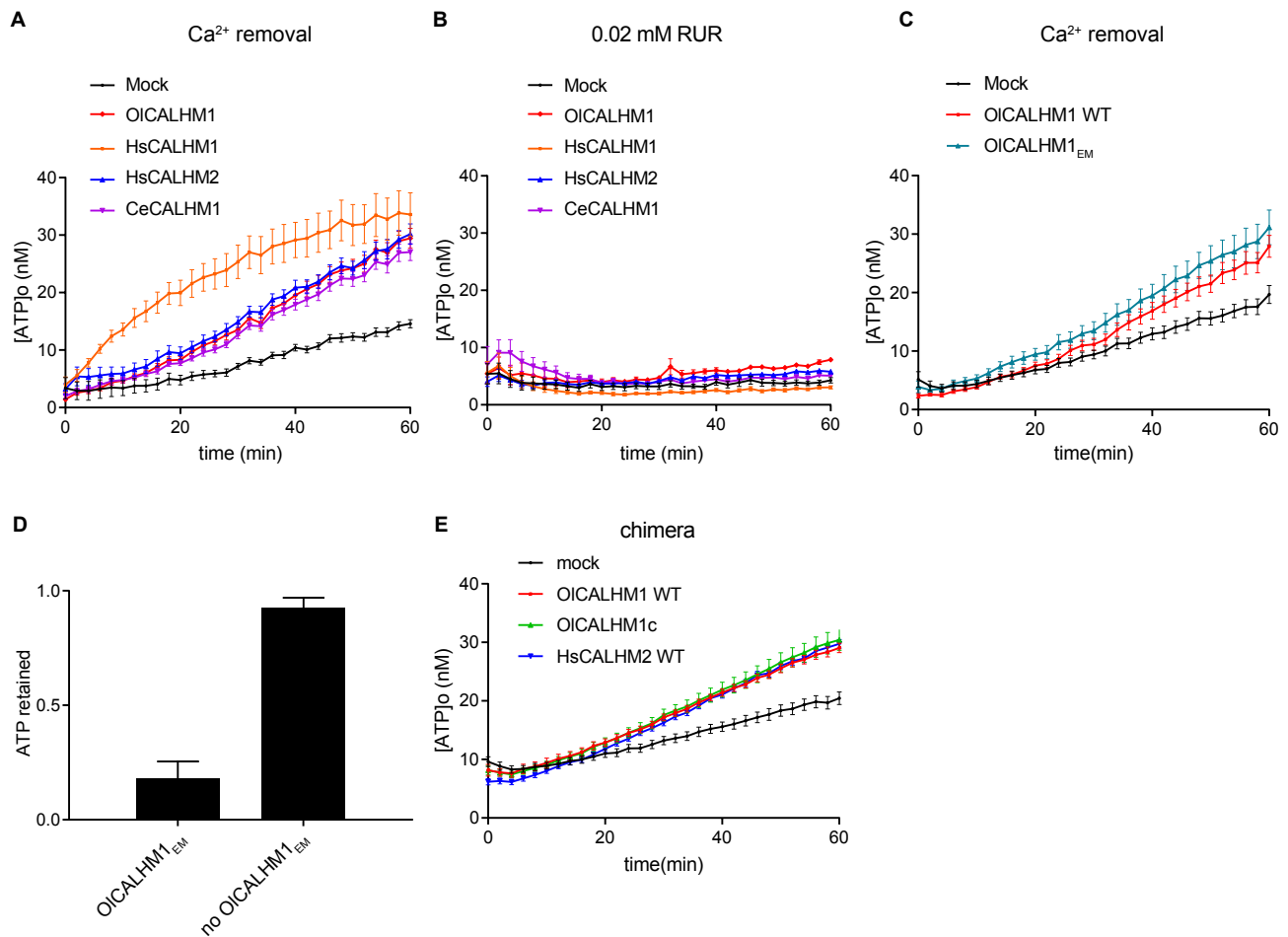


Fig. S2: Functional analyses of the CALHM proteins.

(A and B) Time courses of extracellular ATP levels due to release from HeLa cells transfected with the empty vector (mock), HsCALHM1, HsCALHM2, OICALHM1, or CeCALHM-1 following exposure to essentially zero $[Ca^{2+}]_o$ (17 nM), in the absence (A) or presence (B) of RUR (20 μ M). Data are displayed as means \pm S.E.M. (standard error of the mean) ($n = 8$). (C) Time courses of extracellular ATP levels due to release from the empty vector (mock), full-length OICALHM1, or OICALHM1^{EM} transfected HeLa cells, following exposure to essentially zero $[Ca^{2+}]_o$ (17 nM). Data are displayed as means \pm S.E.M. ($n = 8$). (D) Permeability of the purified OICALHM1^{EM} protein to ATP. Liposomes and OICALHM1^{EM} proteoliposomes loaded with 1 mM ATP were fractionated on the size exclusion column to separate the free extraliposomal ATP from the ATP retained inside. The retained ATP was measured by luminescence using a luciferin/luciferase assay, as the difference between total ATP (inside plus outside, measured after the addition of Triton X-100 to 0.4%) and extraliposomal ATP (before Triton X-100). Data are displayed as the means \pm S.E.M. ($n = 3$) of the ATP retained/total counts. (E) Time courses of extracellular ATP levels due to release from the empty vector (mock), full-length OICALHM1, OICALHM1c, or HsCALHM2 transfected HeLa cells, following exposure to essentially zero $[Ca^{2+}]_o$ (17 nM). Data are displayed as means \pm S.E.M. ($n = 36$).

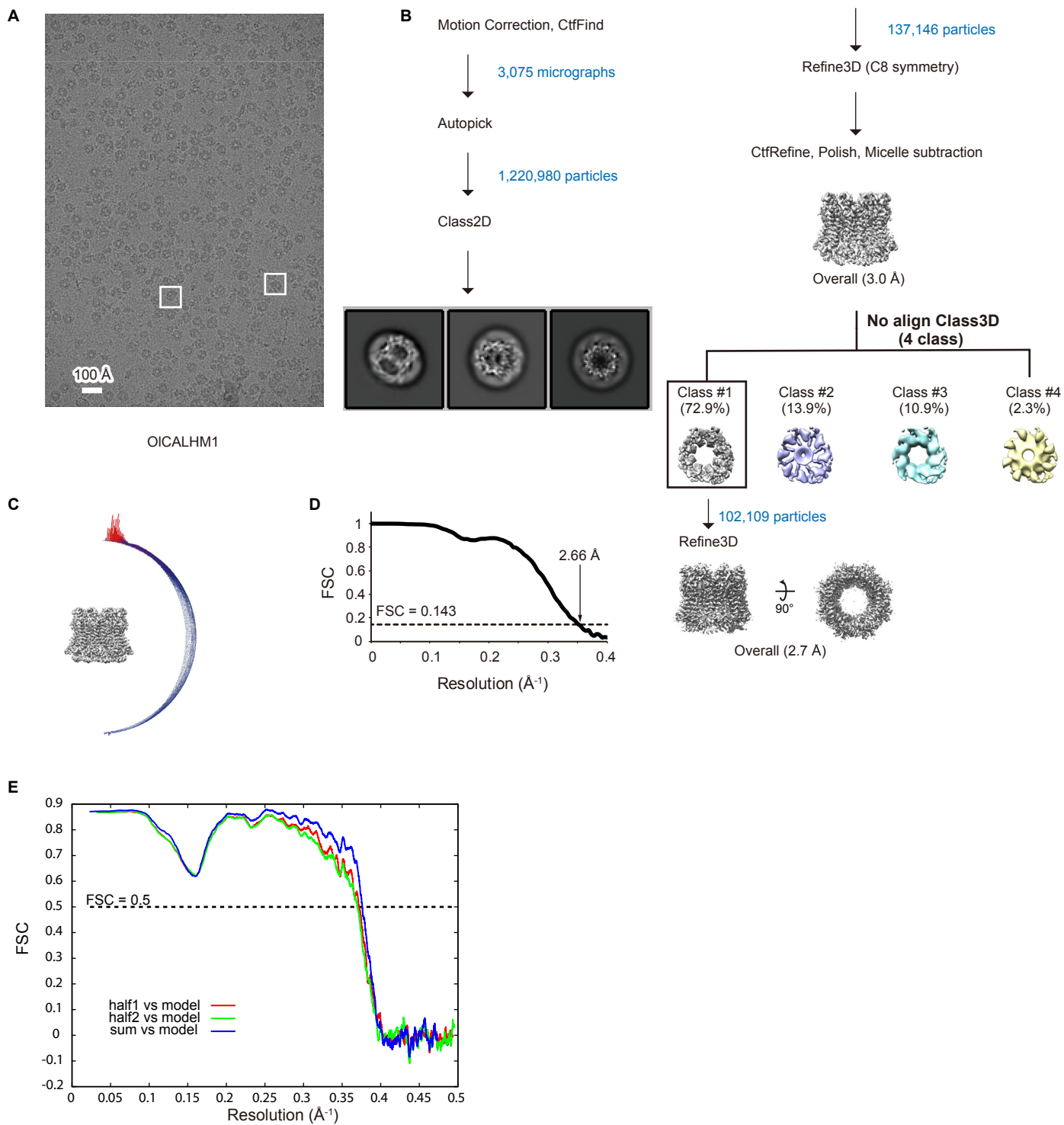


Fig. S3: Cryo-EM analysis of OICALHM1.

(A) Representative cryo-EM image of OICALHM1, recorded on a 300 kV Titan Krios electron microscope equipped with a K3 camera. (B) Image processing workflow of the single particle analysis. (C) Angular distribution. (D) Fourier shell correlation curve of two half-maps. (E) Map-to-model correlation curves.

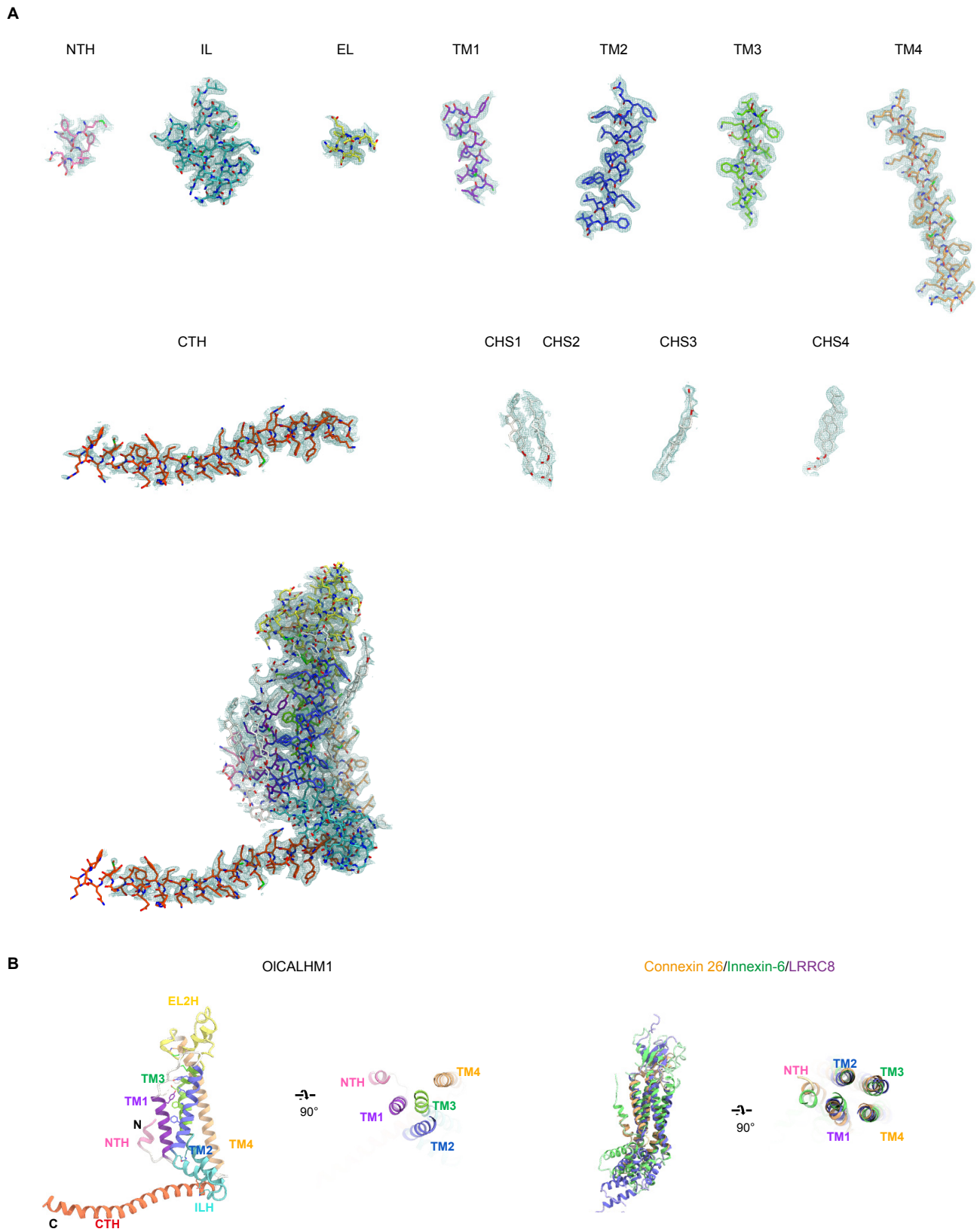


Fig. S4: Atomic model of OICALHM1 in the density maps.

(A) Cryo-EM density and atomic model of each segment of OICALHM1EM. All maps are contoured at 4.0σ . (B) Structural comparison of OICALHM1EM and Gap-like channels (connexin 26, orange; innexin, light green; and LRRC8, purple).

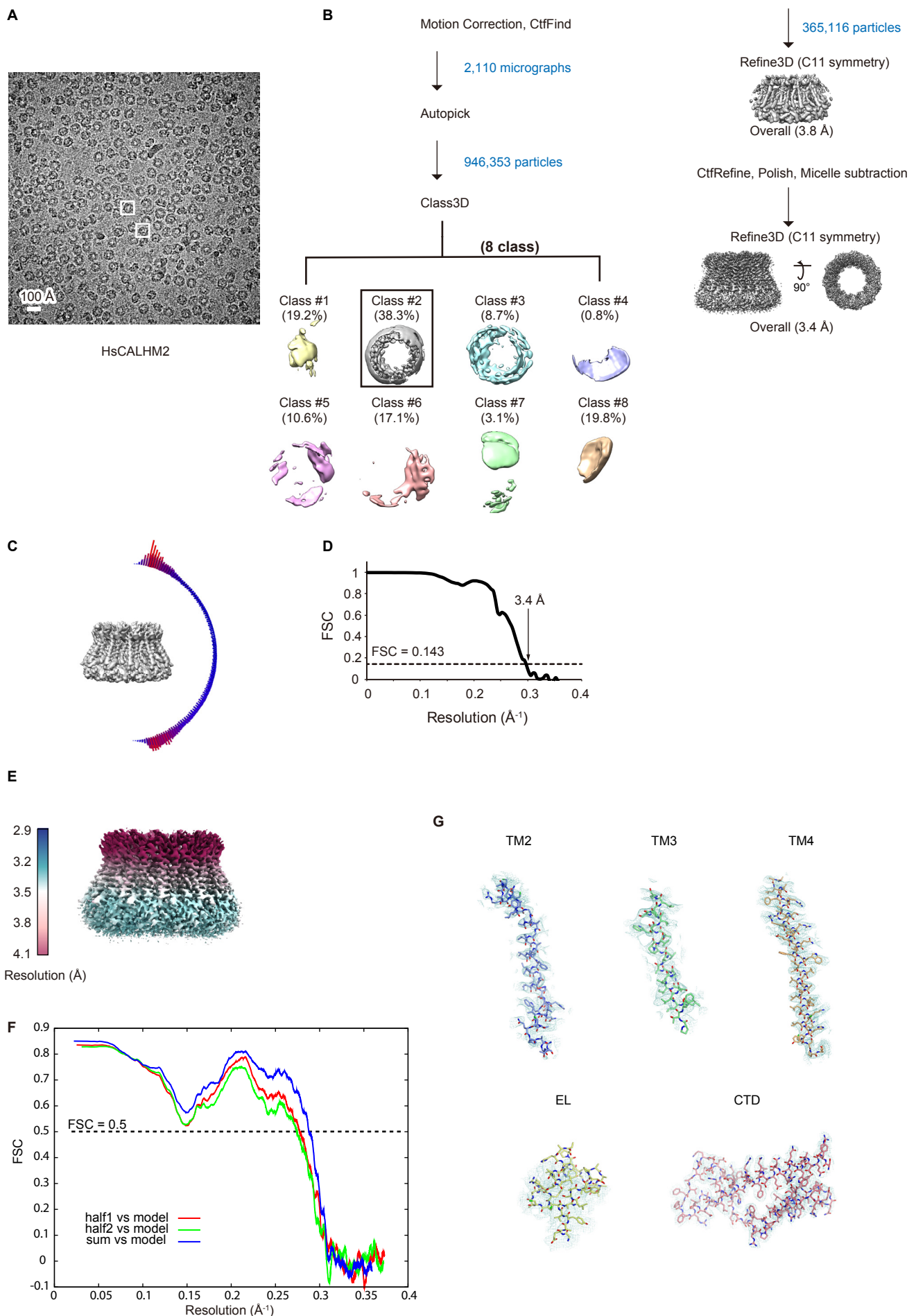


Fig. S5: Cryo-EM analysis of HsCALHM2.

(A) Representative cryo-EM image of HsCALHM2, recorded on a 300 kV Titan Krios electron microscope equipped with a Falcon III camera. (B) Image processing workflow of the single particle analysis. (C) Angular distribution. (D) Fourier shell correlation curve of two half-maps. (E) Local resolution analysis. (F) Map-to-model correlation curves. (G) Cryo-EM density and atomic model of each segment. All maps are contoured at 2.5σ .

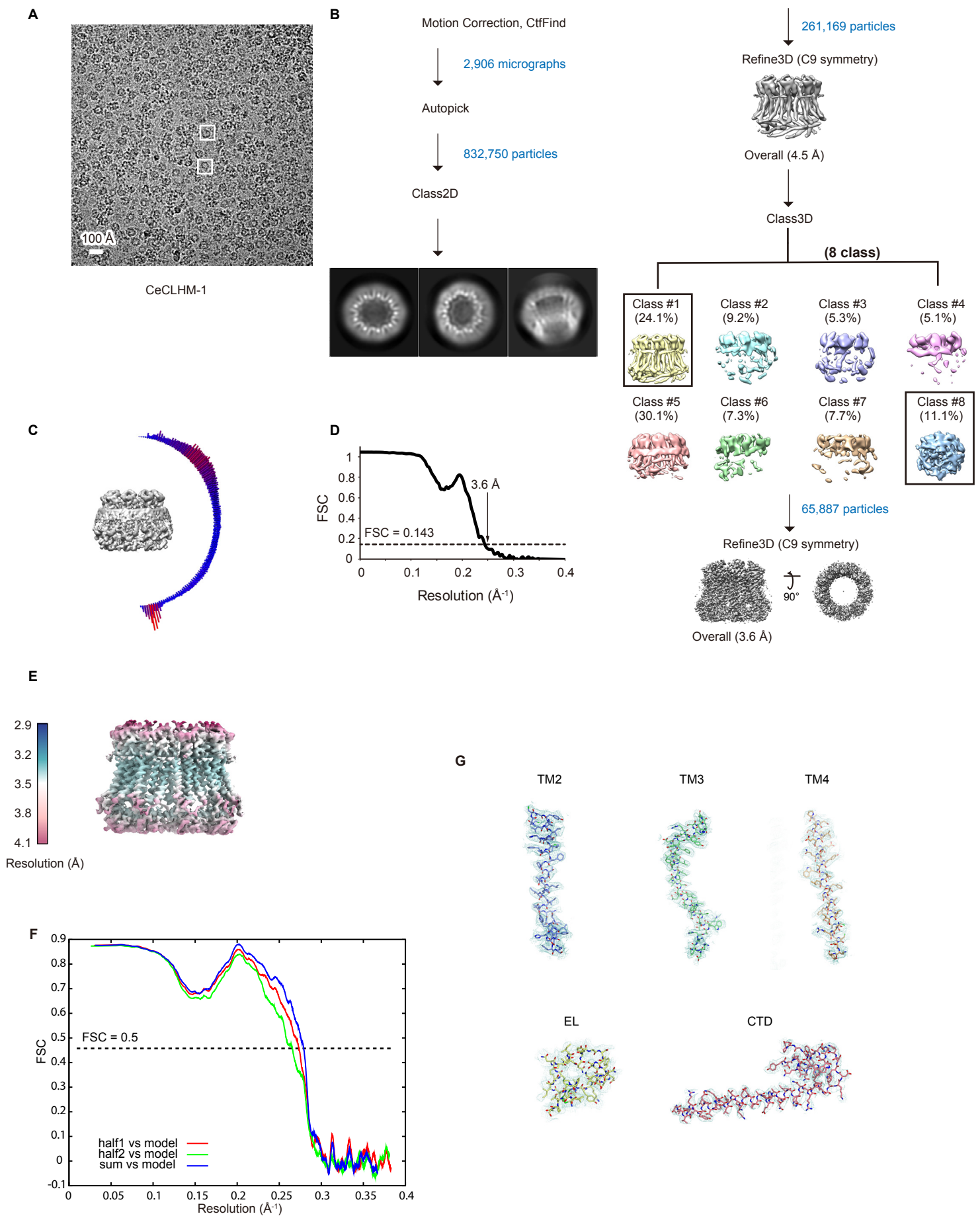


Fig. S6: Cryo-EM analysis of CeCLHM-1.

(A) Representative cryo-EM image of CeCLHM-1, recorded on a 300 kV Titan Krios electron microscope equipped with a Falcon III camera. (B) Image processing workflow of the single particle analysis. (C) Angular distribution. (D) Fourier shell correlation curve of two half-maps. (E) Local resolution analysis. (F) Map-to-model correlation curves. (G) Cryo-EM density and atomic model of each segment. All maps are contoured at 2.5σ .

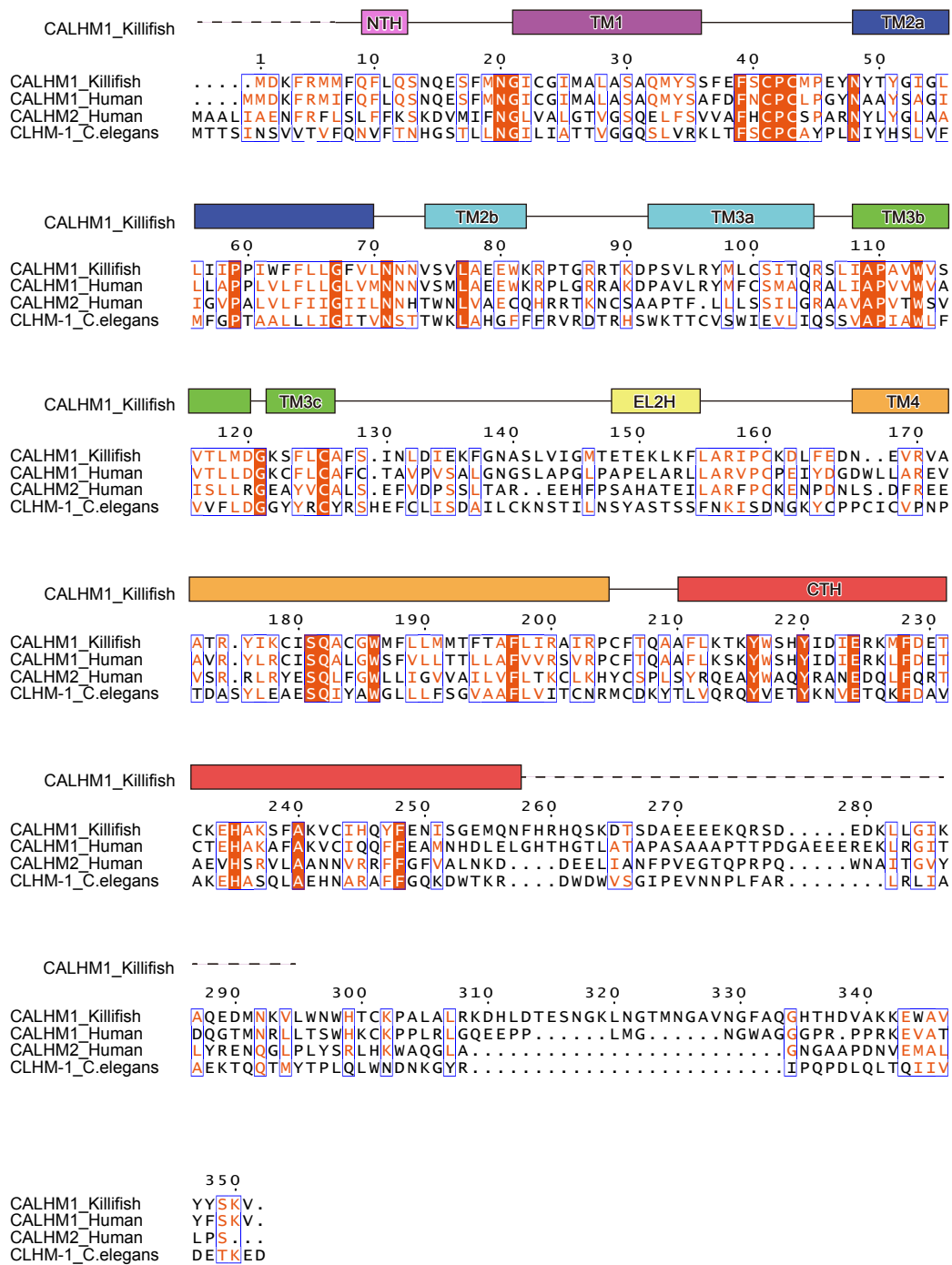


Fig. S7: Amino acid sequence alignment of OICALHM1, HsCALHM2, and CeCLHM-1.

Alignment of the amino-acid sequences of killifish CALHM1 (OICALHM1, UniProt ID: H2MCM1), human CALHM1 (UniProt ID: Q8IU99), human CALHM2 (UniProt ID: Q9HA72), and CeCLHM-1 (UniProt ID: Q18593). Secondary structure elements for α -helices are indicated by cylinders. Conservation of the residues is indicated as follows: red panels for completely conserved; red letters for partly conserved; and black letters for not conserved.

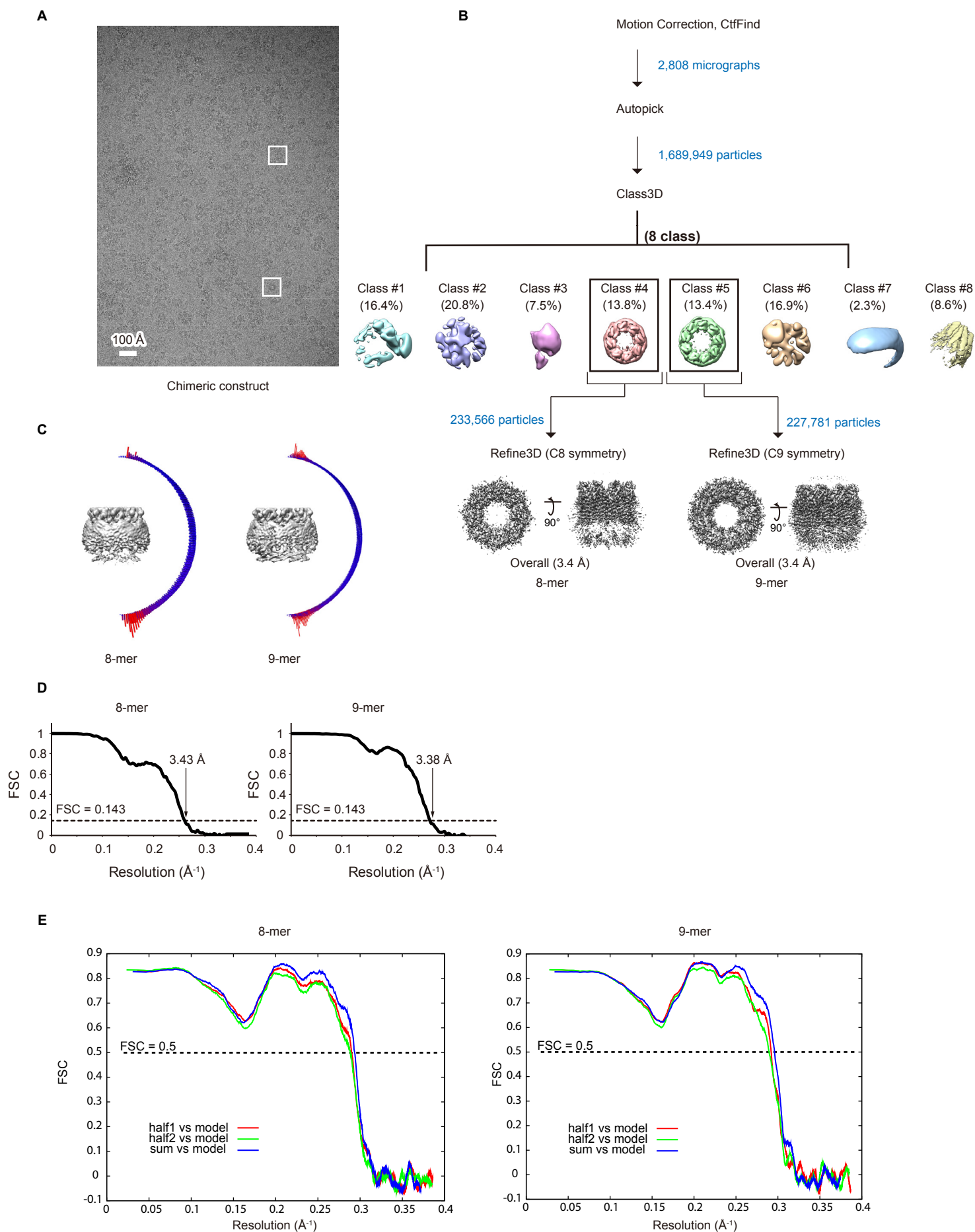


Fig. S8: Cryo-EM analysis of the CALHM chimera.

(A) Representative cryo-EM image of the CALHM chimera (OICALHM1c), recorded on a 300 kV Titan Krios electron microscope equipped with a K3 camera. (B) Image processing workflow of the single particle analysis. (C) Angular distributions of the OICALHM1c 8-mer (left) and 9-mer (right). (D) Fourier shell correlation curves of two half-maps of the OICALHM1c 8-mer (left) and 9-mer (right). (E) Map-to-model correlation curves of the OICALHM1c 8-mer (left) and 9-mer (right).

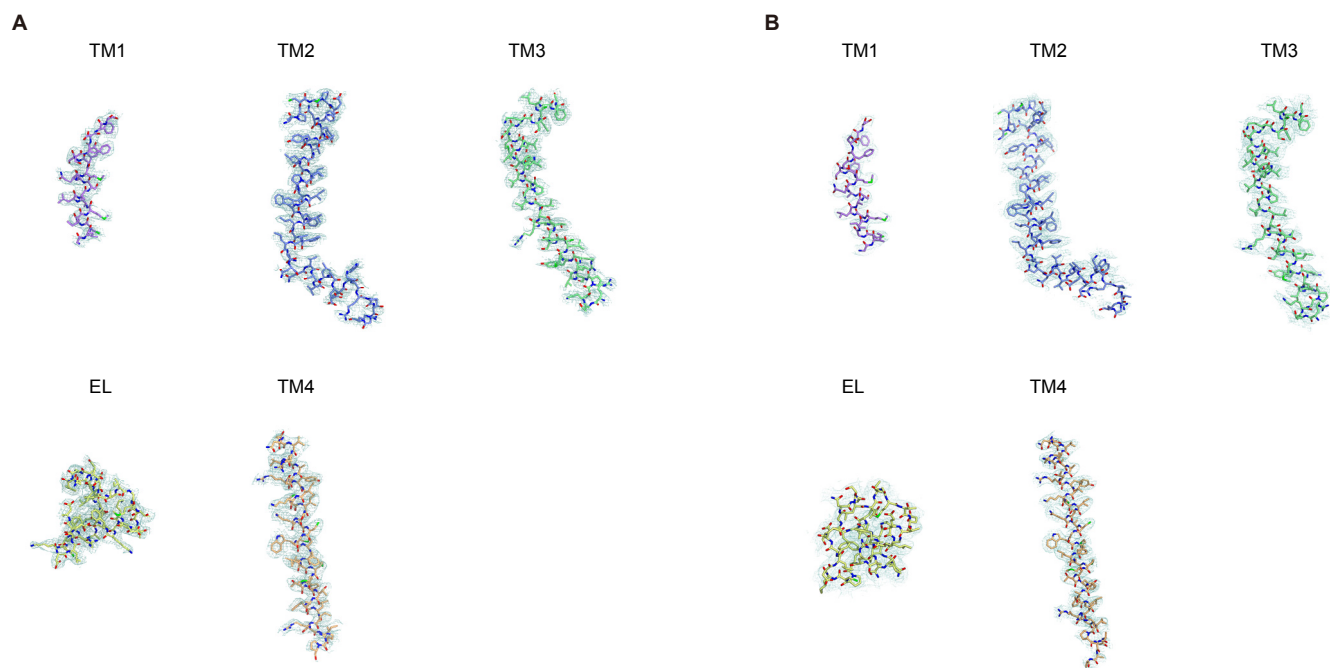
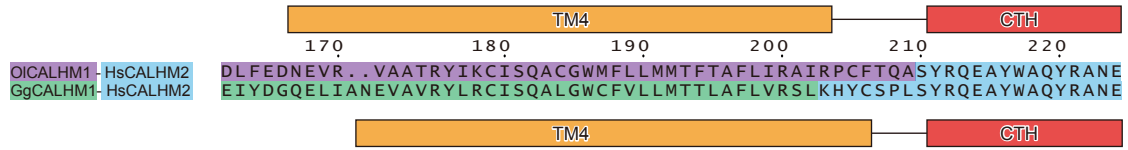


Fig. S9: Atomic model of OICALHM1c in the density maps.

(A) Cryo-EM density and atomic model of each segment of the OICALHM1c 8-mer. All maps are contoured at 2.5σ . (B) Cryo-EM density and atomic model of each segment of OICALHM1c 9-mer. All maps are contoured at 2.5σ .

A



B

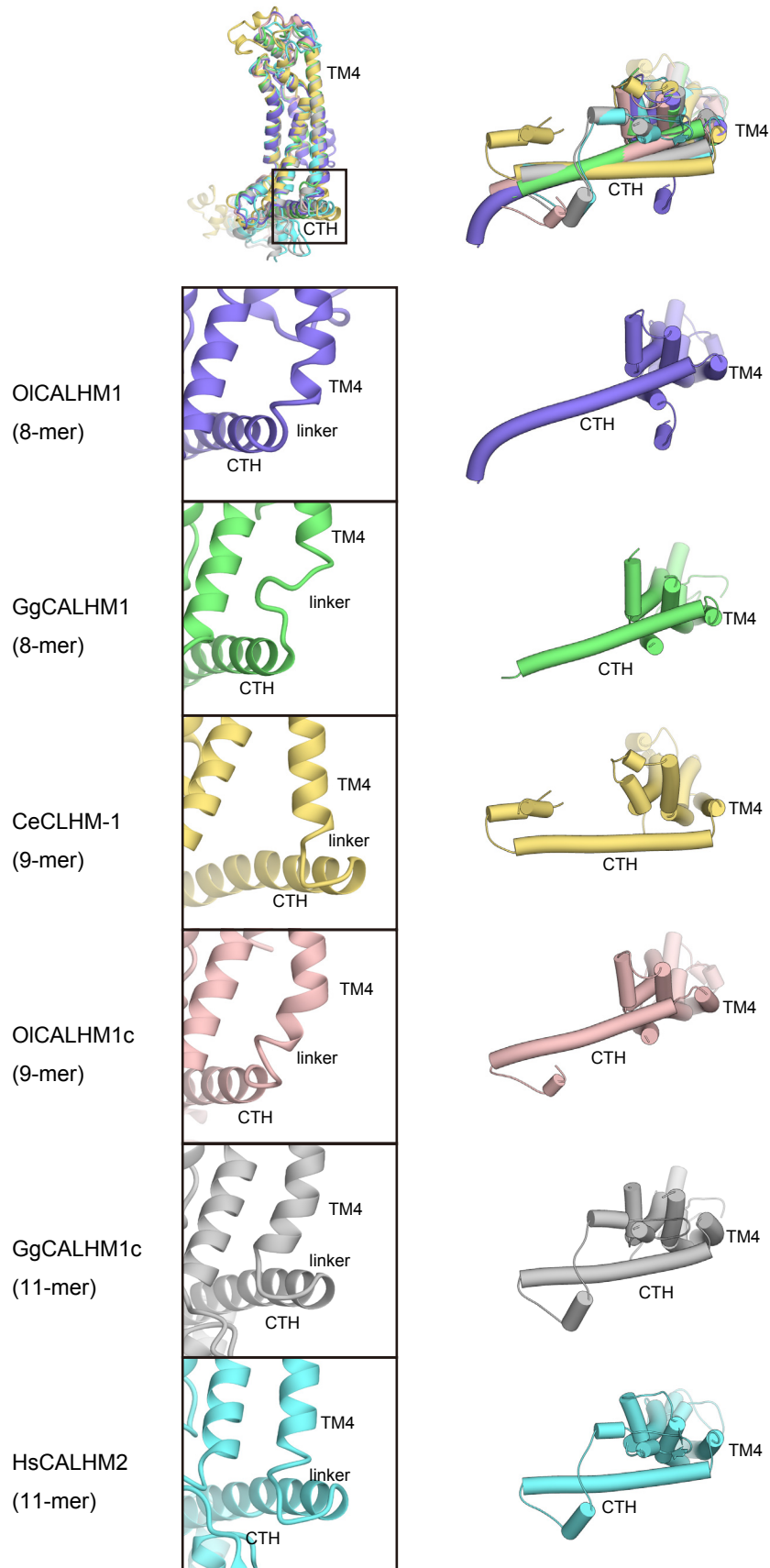


Fig. S10: Structural comparisons with reported CALHM channel structures.

(A) Alignment of the amino-acid sequences of OICALHM1c and the reported chicken CALHM1–HsCALHM2, around the TM4–CTD linker regions. The sequences derived from killifish CALHM1, chicken CALHM1, and human CALHM2 are highlighted in purple, green, and cyan, respectively. Secondary structure elements for α -helices are indicated by cylinders. (B) Structural comparisons of OICALHM1, chicken CALHM1 (GgCALHM1), CeCLHM-1, OICALHM1c (9-mer), the reported GgCALHM1–HsCALHM2 chimera, and HsCALHM2. Superimpositions of these structures are shown in the upper column. Views are parallel to the membrane (left) and from the intracellular side (right). Close-up views of the TM4–CTD linker structures in the enclosed regions (left).

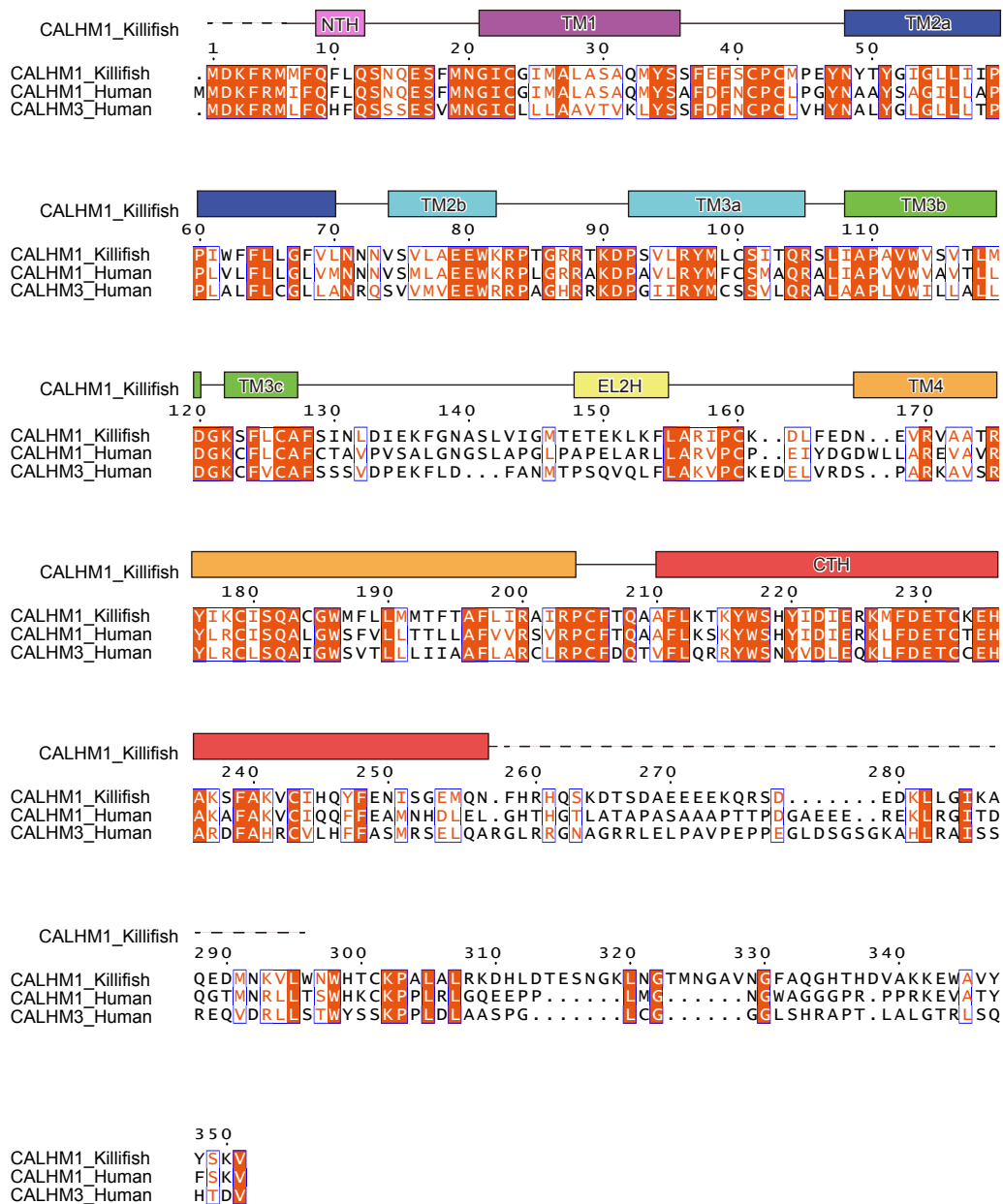


Fig. S11: Amino acid sequence alignment of OICALHM1, HsCALHM1, and HsCALHM3.

Alignment of the amino-acid sequences of killifish CALHM1 (OICALHM1, UniProt ID: H2MCM1), human CALHM1 (UniProt ID: Q8IU99), and human CALHM3 (UniProt ID: Q86XJ0). Secondary structure elements for α -helices are indicated by cylinders. Conservation of the residues is indicated as follows: red panels for completely conserved; red letters for partly conserved; and black letters for not conserved.

Table S1: Cryo-EM data collection, processing, model refinement, and validation statistics.

	OICALHM1 _{EM}	HsCALHM2	CeCLHM-1	OICALHM1– HsCALHM2 chimera (8-mer)	OICALHM1– HsCALHM2 chimera (9-mer)
EMDB ID	EMD-0919	EMD-0920	EMD-0921	EMD-0922	EMD-0923
PDB ID	6LMT	6LMU	6LMV	6LMW	6LMX
Data collection and processing					
Microscope	Titan Krios G3i	Titan Krios G3i	Titan Krios G3i	Titan Krios G3i	
Detector	Gatan K3 camera	FEI Falcon III	FEI Falcon III	Gatan K3 camera	
Nominal magnification	105,000	96,000	96,000	105,000	
Voltage (kV)	300	300	300	300	
Electron exposure (e ⁻ Å ⁻²)	59	60	50	50	
Nominal defocus range (μm)	-0.8 to -1.6	-0.75 to -1.75	-0.75 to -1.75	-0.8 to -1.52	
Pixel size (Å pixel ⁻¹)	0.83	0.8346	0.8346	0.83	
Symmetry imposed	C8	C11	C9	C8	C9
Number of movies	3,075	2,110	2,906	2,808	
Initial particle numbers	1,220,980	946,353	832,750	1,689,949	
Final particle numbers	102,109	365,116	65,887	233,566	227,781
Map resolution (Å)	2.66	3.4	3.6	3.4	3.4
FSC threshold	0.143	0.143	0.143	0.143	0.143
Map sharpening <i>B</i> factor (Å ²)	-61.7	-150	-120.7	-181.1	-184.4
Model building and refinement					
Model composition					
Protein atoms	16,432	22,429	17,766	11,624	15,588
Other atoms	1,120	0	0	0	0
R.M.S. deviations from ideal					
Bond lengths (Å)	0.012	0.010	0.009	0.007	0.019
Bond angles (°)	1.089	1.082	0.909	0.879	1.231
Validation					
Clashscore	4.14	5.34	3.51	2.21	4.67
Rotamer outliers (%)	0.00	1.50	0.94	0.63	1.26
Ramachandran plot					
Favored (%)	97.62	89.27	93.83	98.35	97.90
Allowed (%)	2.38	10.73	6.17	1.65	2.10
Outlier (%)	0.00	0.00	0.00	0.00	0.00